8. FROM DEPTH SCALE TO TIME SCALE: TRANSFORMING SEDIMENT IMAGE COLOR DATA INTO A HIGH-RESOLUTION TIME SERIES

ANDREAS PROKOPH (aprokocon@aol.com)
SPEEDSTAT
36 Corley Private
Ottawa, Ontario K1V 8T7
Canada

R. TIMOTHY PATTERSON (tpatters@ccs.carleton.ca)
Department of Earth Sciences
and Ottawa-Carleton Geoscience Centre
Herzberg Building, Carleton University
Ottawa, Ontario K1S 5B6
Canada

Keywords: Image color time-series, Wavelet transform, Lamination, Sedimentation, Time scale, Depth scale, Varves

Introduction

Requirements and strategy

Line scans of image color from laminated sediments provide an excellent high-resolution tool for the investigation of paleoclimatic and paleodepositional conditions, particularly for Holocene sediments (e.g., Nederbragt and Thurow (2001)). Evidence of orbital and solar activity cycles, oceanic and atmospheric feedbacks in circulation patterns, volcanic activity and plate tectonics, are archived by a variety of means including sedimentary columns, melt layers in ice, tree rings and stalagmite growth-rings (Hays et al. 1976; Berger et al. 1989; Frakes et al. 1992).

It is unfortunately difficult to determine absolute ages for events in many high-resolution geological records, because all such measurements (including image colors) are recorded along a longitudinal axis, or as a depth scale, and not as part of a time scale. Absolute dating techniques such as radiocarbon ^{14}C dating can provide such a time scale, but most available methods require expensive analytical techniques on often rare mineralogical and biotic components in the sediments, and have age uncertainties of $\sim \pm 2\%$ at the 2δ error scale (e.g., Gradstein and Agterberg (1998)). Consequently, radiogenic time-scales cannot

P. Francus (ed.) 2004. *Image Analysis, Sediments and Paleoenvironments*. Kluwer Academic Publishers, Dordrecht, The Netherlands.

resolve most high-frequency changes in sedimentation rates or accretion growth. Thus, by using radiogenic dates, a sediment color time-series that is obtained from line scans can only be scaled to an "averaged" sedimentation rate when developed using a radiogenic time-scale.

Alternatively, laminations (varves) or sediment beds can be counted. For example, identification of sediment color (or gray-scale) contrast in line scans can be obtained from images, or directly from the outcrop. If the time duration of each lamination or bed (e.g., annual) is known, then the lamina/bed thickness provides a measurement of sedimentation rate. Thus, a succession of laminations (or sediment beds) will yield a lamination thickness time series (e.g., Schwarzacher (1993), Varem-Sanders and Campbell (1996)).

Because laminae thickness and laminae (sediment) color can be measured, and the duration of the laminae deposition is known, sediment color from image data represents not only one variable measured in depth-scale, but actually characterizes three different variables: sediment color, sedimentation rate (i.e., varve thickness per year), and time scale (Fig. 1). Variability of sedimentation rate and sediment color can be sensitive to different controlling processes. For example, variability in redox conditions influence sediment color but not the sedimentation rate, while variability in marine productivity may influence the sediment thickness, but not color.

The simultaneous extraction of sedimentation rate and sediment color within a high-resolution time scale can be essential to relate fluctuations in the amount of sediment accumulation to synchronous fluctuations in the environment (e.g., climate change). The following requirements have to be met to accurately extract sediment color and sedimentation rate from a sediment color line-scan:

1) occurrence of a well-defined extraterrestrial cyclicity (e.g., annually due to Earth's rotation around the sun) in the sedimentary succession;

2) sufficient high signal-to-noise ratio of the cyclicity within a sediment image. For example, the signal-to-noise ratio for annual laminations is defined by the ratio of summer-to-winter-color contrast to the background color contrast (measured over the thickness of each annual layer);

3) existence of one or more absolute tie-ages (e.g., radiocarbon ages) for the sediment column.

Earth's orbit around the sun is very regular (i.e., 365.25 days) due to the low friction of Earth's movement with extraterrestrial matter. Thus, the variability in solar irradiance due to variation in the Earth's orbit can be related to the formation of annual varves in lake and marine sediments, annual tree rings, ice melt layers, or ~20,000–100,000 year marine bedding rhythms (Milankovitch 1941). Other, non-orbital extraterrestrial cycles such as the ~11 year sunspot cycle are less useful because of a lack of physical explanation for the narrow bandwidth periodicity in sunspot numbers.

Basically, two techniques permit the automated extraction of laminae from the color contrast in line scans:

1) thresholding; a threshold color value is set (e.g., 125 for medium gray), and all transitions across this threshold are counted (e.g., box-counting technique) and divided by two. This method has the disadvantage that noise that crosses the threshold is also counted and "real" low-contrast laminae may not be counted.

2) edge or inflection point detection; a value of color contrast ("edge") between one or more of the following data points is set (e.g., 100), and all "edges" are counted. This

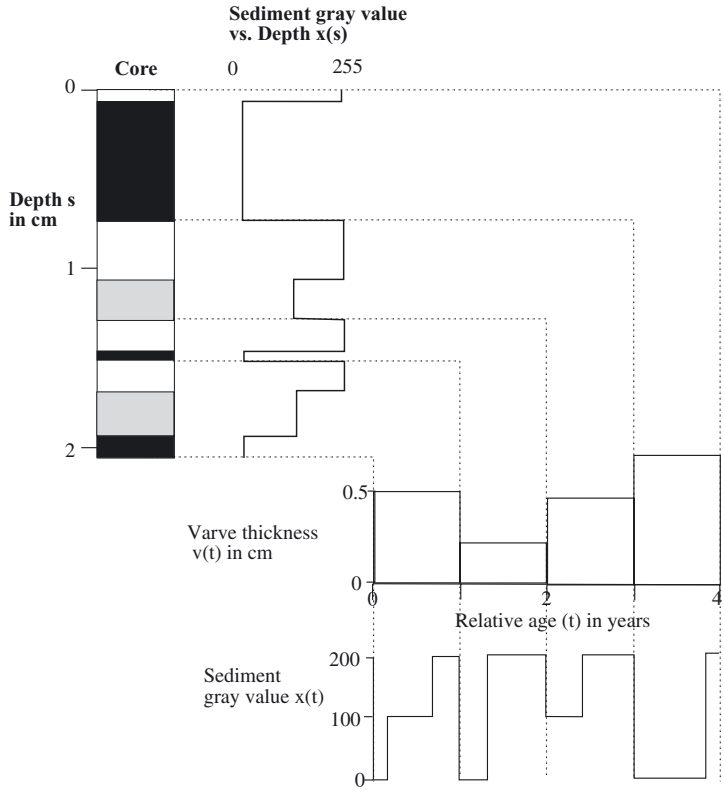

Figure 1. Illustration of different influences of variability in varve thickness (= annual mean sedimentation rate) and variability in sediment gray value in time on their representation in the sediment gray value in a sediment core. Note, that varve thickness and sediment gray-values are not necessarily linked.

method has been used by DendroScan (Varem-Sanders and Campbell 1996) and has the disadvantage that high-frequency noise or sub-seasonal cycles with high contrast may be also counted as lamina, and low-contrast "real" laminae may not be counted.

Aim of study

Here, we present a tuning methodology based on the wavelet transform that detects and extracts in four semi-automatic steps the wavelength of laminae (e.g., varve thickness), sediment color, and generates a time scale based on a sediment color line scan taken at equidistant depth-scale (e.g., pixels from sediment images) (Fig. 2).

In more mathematical terms, the sediment thickness of the complete sedimentary succession, and radiogenic ages t are determined at their sampling depth s, and the average sedimentation rate v is calculated by linear regression. For sediment color time series of

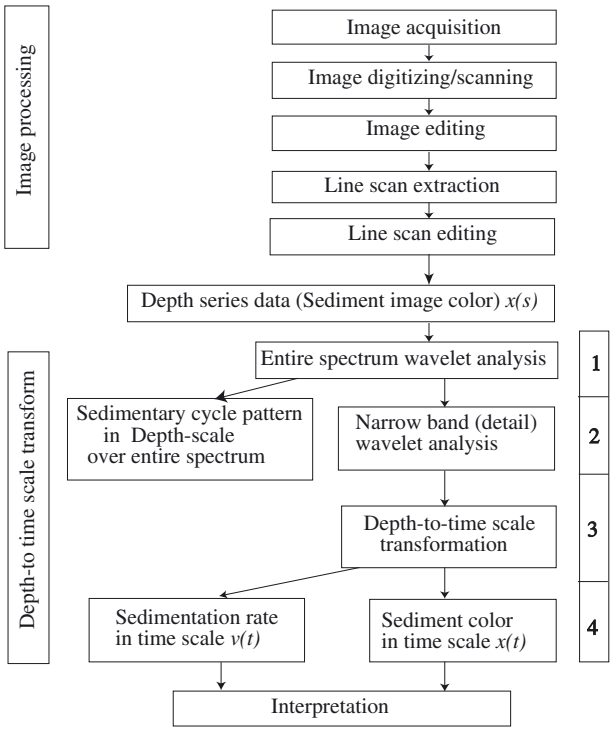

Figure 2. Flow chart of image processing and depth-to-time-scale transform. Note that detailed explanation in the text is restricted to data processing methods. For more details on image processing methods see Schaaf and Thurow (1994) and Nederbragt and Thurow (2001).

laminated sediments, we can measure the sediment thickness s for a number n of annual layers, and sedimentation rates v_i for each individual varve i is

$$v_i = s_i / \Delta t_i \tag{1}$$

with $\Delta t = 1$ yr. Converted to the time domain, each time interval becomes: $\Delta t_i = \Delta s_i / v_i$, and each discrete time point (datum) t_j in a succession of a number n of laminae

$$t_j = t_0 + \sum_{i=1}^{j} \frac{\Delta s_i}{v_i} \tag{2}$$

with $i = 1, 2, \ldots, n$, $j = 1$ to n, and t_0 the absolute age at the top of the time series.

Line scans from sediment images provide discrete data equidistantly in depth (e.g., gray value of pixel) and not in the time domain. In this way a time series $x = f(s)$ of

gray values x at equidistant depth intervals (pixel size) Δs with pixel number r is formed. Consequently, the discrete depth interval Δs is constant and not the time interval Δt. For this reason, the following methodology is proposed to transform all sedimentary signals into an equidistant time-scale.

Before we explain the methodology step by step, we give an introduction to the wavelet analysis techniques used, followed by brief remarks on image processing requirements. The 4-step methodology utilizes line scans obtained from images of laminated sediments, but can also be used for other geological or geophysical (e.g., well-logging) time-series as long as the requirements outlined above are respected. We apply this methodology to a synthetic signal and an example from Holocene marine anoxic sediments with annual lamination (varves). We also show how the method deals with variable sedimentation rates, non-laminated intervals and various types of noise.

Wavelet analysis

Wavelet analysis emerged as a filtering and data compression method in the 1980's (e.g., Morlet et al. (1982)). Since then, it has become widely applied in geophysics (e.g., Grossman and Morlet (1984)). Wavelet analysis transforms information from a "depth" or "time" domain into a spectral domain by using various shapes and sizes of short filtering functions, so-called "wavelets".

In time-series analysis, wavelets permit an automatic localization of periodic-cyclic sequences. In contrast to the Fourier transform that uses a single window of constant width, the wavelet transform uses narrow windows at high frequencies, and wide windows at low frequencies (Rioul and Vetterli 1991). The wavelet coefficients W of a time series $x(s)$ are calculated by a simple convolution

$$W_\psi(a,b) = \left(\frac{1}{\sqrt{a}}\right) \int x(s)\psi\left(\frac{s-b}{a}\right) ds, \tag{3}$$

where ψ is the mother wavelet; the variable a is the scale factor that determines the characteristic frequency or wavelength; and b represents the shift of the wavelet over $x(s)$ (Chao and Naito 1995). Alternatively, $\sqrt{a}$ can be replaced by a, the so-called L1-norm, which calculates W comparable to the power in spectral analysis (i.e., variance).

In this contribution, we have utilized a continuous wavelet transform, with the Morlet wavelet as the mother function (Morlet et al. 1982). The Morlet wavelet is simply a sinusoid with wavelength/period a modulated by a Gaussian function, and has provided robust results in analyses of climate-related records (Prokoph and Barthelmes 1996; Appenzeller et al. 1998; Gedalof and Smith 2001). A parameter l is used to modify wavelet transform bandwidth-resolution either in favour of time or in favour of frequency, and represents the length of the mother wavelet or analysis window. The bandwidth resolution for wavelet transform varies with $\Delta f = \frac{\sqrt{2}}{4\pi a l}$, and a location resolution $\Delta b = \frac{al}{\sqrt{2}}$. The parameter $l = N\Delta t = 10$ is suggested for all analyses, which give sufficiently precise results in resolution of depth and frequency, respectively (Prokoph and Agterberg 2000; Ware and Thomson 2000). Thus, the shifted and scaled Morlet mother wavelet is defined as

$$\psi^l_{a,b}(s) = \pi^{-\frac{1}{4}}(al)^{-\frac{1}{2}} e^{-i2\pi\frac{1}{a}(s-b)} e^{-\frac{1}{2}(\frac{s-b}{al})^2}. \tag{4}$$

The relative bandwidth error is constant in all scales and is $\sim 1/10 = 0.1$ (=10%) for $l = 10$. For example, a varve thickness of 1 cm has an error of ± 0.1 cm. The value $l = 10$ also diminish effects of local artefacts or non-laminated sediment parts in the images. Several possibilities to adjust the width, types and other characteristics of mother wavelets that are similarly useful to perform the depth-to-time transform successfully are presented in Torrence and Compo (1998). Figure 3 illustrates the real part of the complex Morlet wavelet with the parameters used and the relative analysis window size used depending on depth and wavelength.

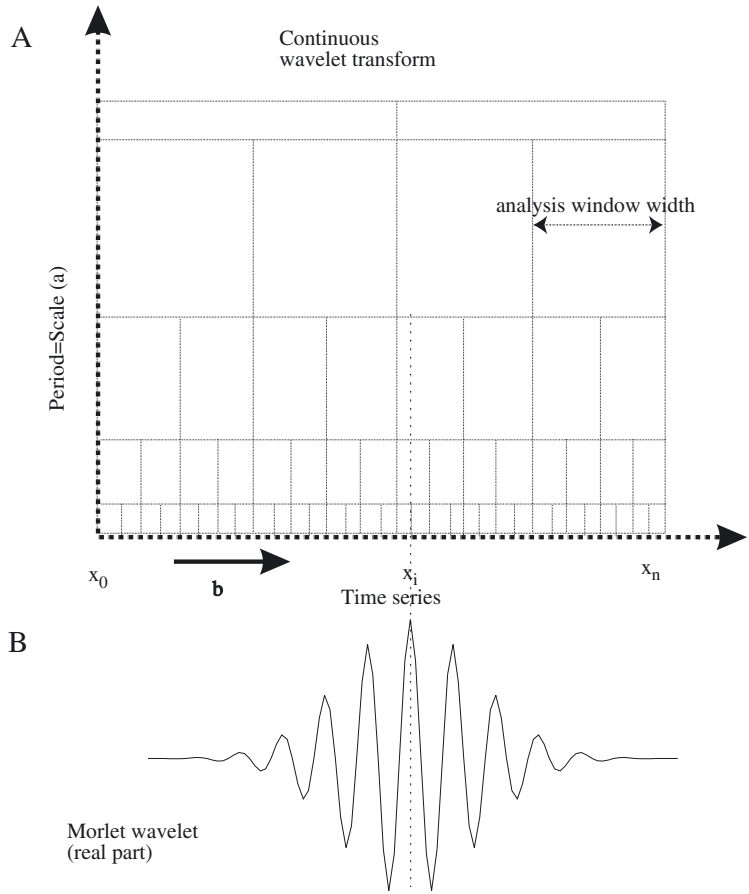

Figure 3. Schematic presentation of (A) simplified analysis windows for continuous wavelet analysis including (B) real part of Morlet wavelet centered at location x_i. For explanation of the axis a, b as well as x_0 see equation (3) in text.

The wavelet coefficients on the top and bottom of the data set have an "edge effect", because only a half of the Morlet wavelet lies inside the line-scan data set, and the missing

data in the analysis windows are replaced ("padded") by zeros. The missing data can be up to 50% of the analysis window. Thus, for relatively long wavelengths (e.g., wavelength a covers more than a half of the whole data series), the edge effect decreases to zero as soon as data points cover the complete analysis window. The boundary of edge effects on the wavelet coefficients forms a wavelength dependent curve, called the "cone of influence" (Torrence and Compo 1998). Wavelet coefficients for wavelengths (or scales) longer than the borderline of the cone of influence become less significant. However, since the data set used for bandwidth wavelet analysis generally consists of many laminae, in the high-frequency variations, the influence of edge effect at $l = 10$ covers not more than 5 laminae both on top and bottom.

To transform a measured and hence limited and discrete time-series, the integral in equation (3) has to be modified by using the trapezoidal rule to evaluate the wavelet transform (Prokoph and Barthelmes 1996). The matrix of wavelet coefficients $W_l(a, b)$ can be coded with the appropriate colors or shades of gray for graphical expression, using a "scalogram". In our examples, we used shades of gray, with black representing 75–100%, dark gray 50–75%, light gray 25–50%, and white 0–25% of maximum $W_l(a, b)$. Wavelet transform using the Morlet wavelet can be performed with several software packages (e.g., MATLAB®; Prokoph and Barthelmes (1996), Torrence and Compo (1998)). The wavelet analysis technique used in this article is explained in detail in Prokoph and Barthelmes (1996).

The series of wavelength $a_{\mathrm{wmax}}(b)$ with strongest local wavelet coefficient $W_l(a, b)$ has to be extracted from the wavelet coefficient matrix, because this series of wavelengths determines the lamination thickness at each location. For example, the output-file can provide the depth-scale (1st column) and the lamination thickness (2nd column). The extraction of $a_{\mathrm{wmax}}(b)$ can easily be performed with a search algorithm for "maximum" in a spreadsheet.

Image processing

Sediment color line scan data can be acquired, for example, from photographs of cut or rough sediment surfaces, thin section photographs, Backscattered Electron Microscope (BSEM) photographs, or X-ray imaging. The quality, resolution, costs and color calibration of these imaging techniques varies significantly. Figure 4 illustrates how different resolution and image acquisition techniques can enhances/ smooth contrasts in sediment color, and that very-high resolution and high-cost images (i.e., BSEM) are not necessarily optimal for automatic counts of varves. The photographs can already be in digital format, or may be transferred to digital (electronic) format after scanning (Lamoureux and Bollmann, this volume). The most common, and due to low compression, recommended high-quality digital files are TIFF-files, but several other bitmap-file formats are also useful. Several image processing software packages such as NIH-Image (for Macintosh), IMAGEJ (for all platforms), or XVIEW (UNIX) are suitable for extracting and editing sediment color line scans from digital sediment images. Variations in the image background color should be calibrated to equal standard value by using trend lines according to Nederbragt and Thurow (2001). In this way, errors in the sediment color (e.g., slightly different core diameter, or X-ray intensity fluctuations) can be corrected.

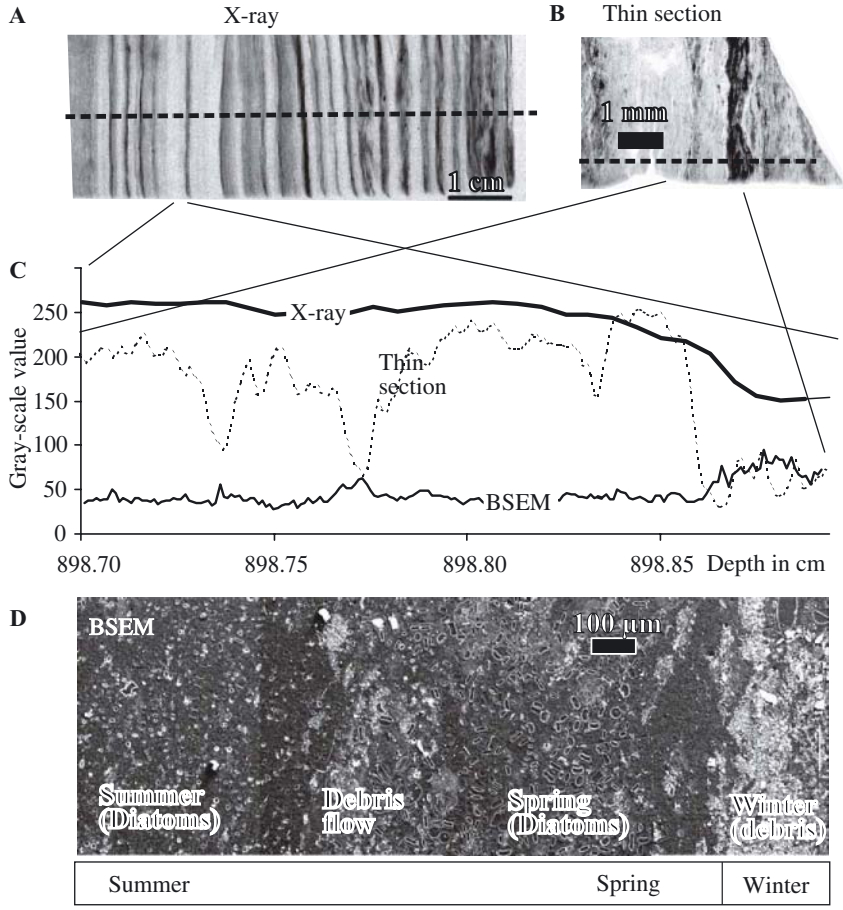

Figure 4. Graphic correlation of digital image output from 898.7–898.89 cm depth of core TUL99B-03, Effingham Inlet, west coast of Vancouver Island (after Patterson et al. (2001)). A) X-ray image (1 cm = 116 pixels, line-scan width: 3 pixels); B) Thin section image (resolution: 1 cm = 1000 pixel, line-scan wide: 40 pixel); C) Line-scan outputs of sediment color (gray value); D) BSEM image (resolution: 1 cm = 12, 500 pixels, line scan wide: 400 pixels), diatoms are represented by bright colors in X-ray and thin section (gray-scale value >200) and debris layers by dark colors (gray-scale values <100). Note that the correlation of the line scans is almost perfectly positive or negative, but varve detection of X-ray images is not suppressed by thin sub-annual debris layers.

Mean gray values are then measured for several pixel line scans that perpendicularly cross the sediment lamination from each image, and are saved as an ASCII file in two columns (pixel number, gray value). Further editing of all line scans involves correcting depth values from pixel numbers, replacement of extreme gray values, e.g., due to small cracks or concretions, by using adjacent gray values (after Schaaf and Thurow (1994)), and connecting the time-series data of each image to a complete data set for the entire core.

The pixel size has to be calibrated with a depth scale, which is photographed or scanned together with the sediment column (e.g., Nederbragt and Thurow (this volume)).

Methodology

Determination of the range of lamination (e.g., varve) thickness from the line-scan time-series is carried out by using the wavelet analysis with program CWTX.F, or other automatic techniques (e.g., Varem-Sanders and Campbell (1996)). By using wavelet analysis over the entire spectrum of wavelength (pixel range from 2 to r), the lamination thickness range is marked by grey or black bands in the wavelet scalogram. It is important that a useful signal-to-noise ratio exists in the raw image; in particular a strong contrast between the summer and winter layers (varves). For very noisy sections (signal-to-noise ratio smaller than 1 to 1) and interbedded sections with completely missing laminae, it is recommended that the range of lamination thickness (measured in distance units such as pixel, mm, cm) determined manually from the images, or from the line scan.

Narrow bandwidth wavelet analysis of the sediment color data $x(s)$ is performed in the range of lamination thickness bandwidth determined by the previous step. By narrowing the bandwidth of the range of varve thickness in a section, high-frequency noise ("white noise"), as well as overlying long-term sediment color variability are removed in the wavelet coefficients. The user defines the number of depth-intervals m for which the varve thickness is extracted before or during the run of the wavelet analysis software used. The number of depth-intervals should be $m > S^*2/\nu_{\min}$ with $\nu_{\min}$ defining the minimum varve thickness. The depth interval is $\Delta s = S/m$. Consequently, the absolute depth of each interval k is defined by $s_k = s_0 + \Delta s^* k$, with s_0 representing the depth at the top of the time-series. The wavelength with the highest variance at location s_k determines the local sedimentation rate (i.e., varve thickness) ν_k that is extracted by the wavelet analysis software in the second column of output file. T is sediment color x_k for each depth s_k at the same Δs can then be calculated using a simple linear data interpolation algorithm to extract three new time series ν_k, x_k, s_k in depth-scale with equidistant Δs. Here, we use MITTELN.C for UNIX to construct equidistant time series that is downloadable from http://www.geocites.com/speedstat/MITTELN.C.

To obtain an absolute rather than relative time-scale, a tie age t_p at depth s_p has to be provided from an independent source (e.g., radiogenic age, bio- or litho stratigraphic marker age) for calibration. If there is no independent age available, the new time series can still be used for evaluation of environmental processes, but cannot be linked to other records. The absolute datum t of each lamination at depth interval $k = 1 \ldots n$ can then be calculated to yield time-scale data t_k by

$$t_k = t_p + \sum_{i=1}^{k} \frac{\Delta s}{\nu_i} \qquad \text{for } \Delta s^* k + s_0 > s_p \tag{5.1}$$

and

$$t_k = t_p - \sum_{i=1}^{k} \frac{\Delta s}{\nu_i} \qquad \text{for } \Delta s^* k + s_0 < s_p. \tag{5.2}$$

These calculations can be done with a simple spreadsheet, for example in MS EXCEL®. By this stage, an absolute depth s_k, a sediment color value x_k, a varve thickness ν_k, and an absolute "counted", but non-equally spaced time t_k has been extracted for each depth interval $k = 1 \ldots m$.

Finally, the equal-distance data (Δs = constant) s_k, x_k, ν_k, t_k is transformed into n equidistant time intervals with Δt = constant using a simple linear interpolation algorithm (i.e., MITTELN.C) to yield s_i, x_i, ν_i, t_i. Note, that $\Delta t = 1$ year is the highest possible resolution for the varve thickness time series ν_i. The highest possible time-resolution Δt for the sediment color x is $\Delta t = (t_n - t_0)/r$. This resolution is usually much higher (i.e., by the number of pixel per varve) than the highest possible resolution for sedimentation rate (= varve thickness).

Testing of the method

Synthetic signal

To illustrate such a combined statistical approach, we introduce here a synthetic signal (Fig. 5) to demonstrate that the methodology is able to resolve the original climate signals and fluctuations of sedimentation rate from a complex sediment color depth-series. This synthetic signal combines following features:

1) $A(t) = (2\cos(2\pi t/20) + 50)^*(5\cos(2\pi t) + 5)$ calculated for $t = 1 \ldots 500$ and $\Delta t = 0.25$ year. This signal simulates sediment color (gray scale) variations in a range from 30 (dark) to 70 (brighter), and maximum amplitude of up to 40, with four pixels covering 1 year intervals. This signal represents low-contrast-laminae stages (e.g., no winter-summer precipitation difference = zero annual amplitude) and high-contrast-laminae stages (e.g., strong seasonal precipitation contrast = annual amplitude of 40 gray values).

2) $B(t) = 2\cos(2\pi t/50) + 50)$ calculated for $t = 1 \ldots 500$ and $\Delta t = 0.25$ year. This signal may represent a long-term cyclicity in the record (e.g., sunspot cyclicity) (Fig. 5B).

3) $C(t) = 10^*\varepsilon$ calculated for $t = 1 \ldots 500$ and $\Delta t = 0.25$ year. This signal represents white (random) noise ε with amplitude of up to 10 that can arise from random geological processes as well as limitations in the image quality (Fig. 5C).

4) $D(t) = A(t) + B(t) + C(t)$. Thus, the different time-series signals (A), (B), (C) are added over 500 years. The units for $A(t)$, $B(t)$, $C(t)$, and $D(t)$ are gray value units (Fig. 5D).

5) $E(t) = 20\cos(2\pi t/20.25) + 20.5$ calculated for $t = 1 \ldots 500$ and $\Delta t = 0.25$ year. This signal represents a 20.25 year-cosinusoidal variation on sedimentation rate $\nu(t)$ with amplitude of 20.5 to 60.5 (average: 40.5), with unit for $E(t)$ in mm/year (Fig. 5E).

6) The final sediment color signals $x(s)$ is related to a depth-scale by time-scale to depth-scale transform $s(t) = s(t-1) + E(t)^*\Delta t, s(0) = 0, t = 1 \ldots 2000$ and $\Delta t = 0.25$ year. The transformed synthetic signal time series is 20318 mm long (Fig. 6A1, A2) with an amplitude range $x(s)$ of 85 to 130 units (i.e., gray values). By simple linear interpolation the time series $x(s)$ is stretched to 20000 data points in equidistant depth and provides an assumed image resolution of $\Delta s = \sim 1$ pixel/mm.

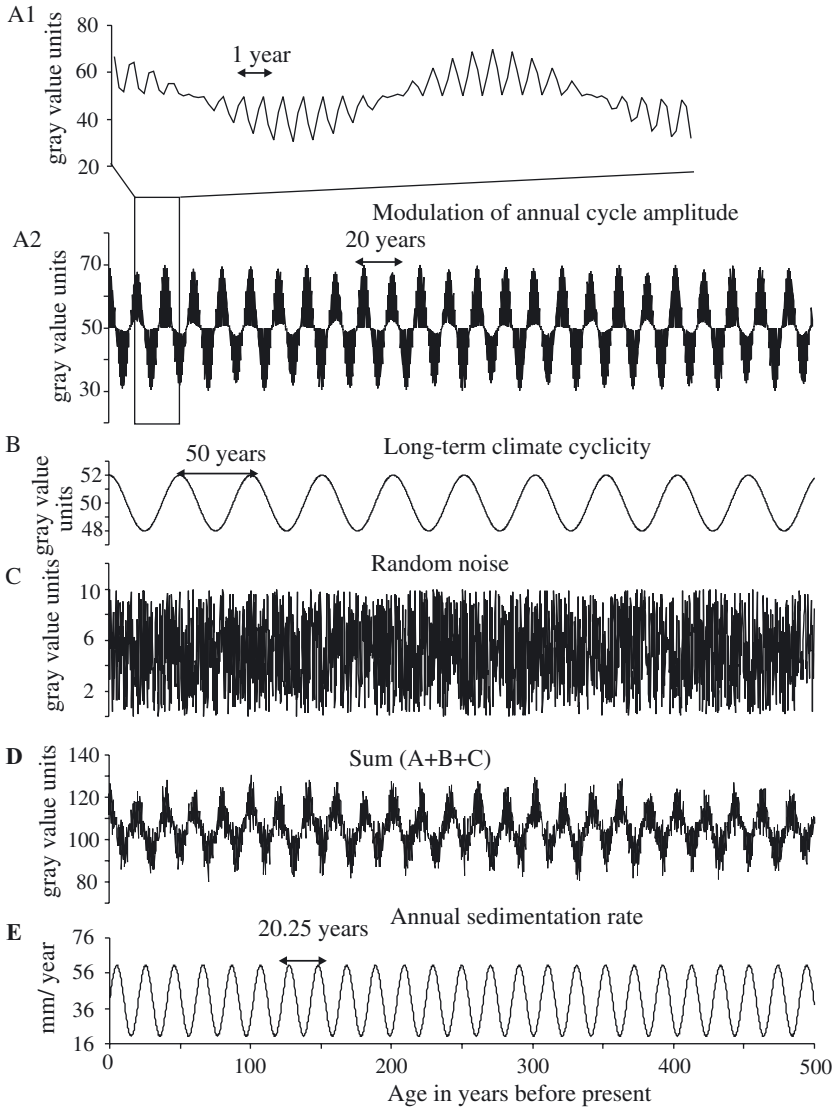

Figure 5. Synthetic time-series for signals over 500 years embedded in sediment image color line-scan. Vertical scale: Sediment gray-value. For details on construction of the signals A1, A2, B, C, E, see text. Note that (A2) is a zoom into (A1).

Table 1. CWT-output of narrow-band analysis of synthetic signal.

Raw (k)	Depth (mm)	$W_{\max(b)}$ varve thickness	Age (years)
	1.00		$T_0 = 0$
1	11.16	58.48	0.17
2	21.32	58.48	0.35
3	31.47	58.48	0.52
4	41.63	58.48	0.69
$k = 5$	s_5	ν_5	T_5
k	s_k	ν_k	T_k
$k = 1995$	s_{1995}	ν_{1995}	T_{1995}
1996	20276.37	62.87	491.25
1997	20286.53	62.87	491.41
1998	20296.68	62.87	491.57
1999	20306.84	62.87	491.73
$m = k = 2000$	20317.00	62.87	491.89

The depth-scale to time-scale transform of the synthetic signals

The wavelet analysis of the depth series $x(s)$ show wavelet coefficients with >25% of maximum variance in shades of gray (Fig. 6B, C).

In the overview analysis (Fig. 6B), a very strong ~800 mm cycle band, a highly fluctuating ~20 to 60 mm, and weaker ~400 mm and ~2000 mm bands emerge. From the synthetic signal (Fig. 5E) with an average sedimentation rate of ~40 mm/year, we can conclude that these cycles represent ~20 years, ~1 year, ~10 years and ~50 years. However, it is not possible to separate the components of the ~20 year cycle that belong to the sedimentation rate and climate cycle fluctuations, respectively. The ~10 year cycle is not in the model, and thus may represent a bandwidth error effect that is inherited in the analysis methodology. Since this work refers to the analysis of images, we can, generally conclude that the ~20–60 mm cycle band represents the annual lamination variation.

In the detailed wavelet analysis (Fig. 6C), we separate the 5–200 mm band to cover the annual cycle band and give some space to possible unusually thick or thin laminae ("outliers"). There are no outliers in the synthetic signal, but they are common in sedimentary time-series.

The wavelength of the strongest local signal $a_{\mathrm{W}\max(s)}$ for each depth interval b (column 3) (Table 1), which represents the sedimentation rate ν_k is extracted in a numerical output file of the wavelet analysis. Then, according to equations (5.1) and (5.2), the time scale is calculated as a function of depth (column 4, Table 1). Here, we use a tie-age $t_p = 0$ years BP at 0.0 mm. The first step of the transform shows that the recovered time scale ranges from 0–491.8 yr. BP., that is 1.8% shorter than the original time scale.

Now, mean gray-value data x for the intervals $k = \Delta s$ are calculated, and x_k is attached as column 5 to the time scale. Then, the time scale T, sedimentation rate ν, and signal (sediment color) x are transformed from equidistant depth intervals k to equal time intervals

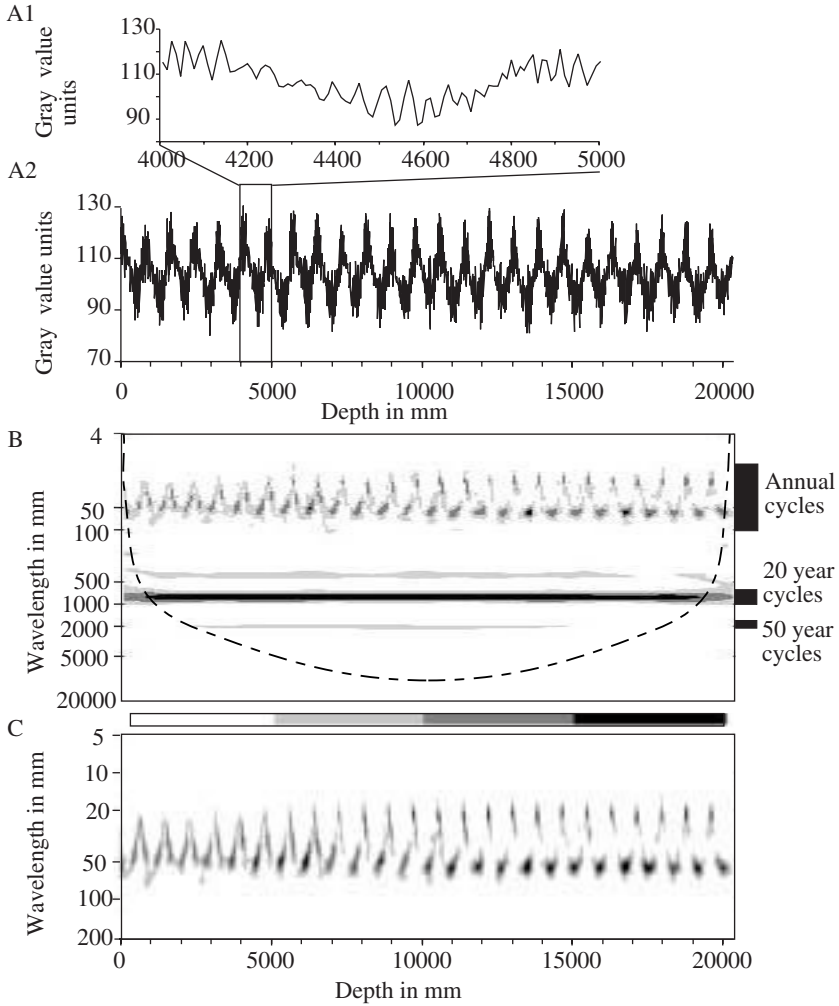

Figure 6. Time-series analysis of synthetic signals of periodic signals and noise (Fig. 5E) modulated by annual sedimentation rate (Fig. 5F). A1: Zoom into 1000 mm interval of synthetic signals transformed from time to depth scale; A2: complete 20000 m of synthetic time-series (e.g., sediment color line scan from image); B: Scalogram of the wavelet analysis over the complete spectrum of the synthetic signals using Morlet wavelet with 10 oscillations; stripped line marks "cone of influence' of edge effects; C: Scalogram of the narrow bandwidth wavelet analysis of synthetic time-series in depth scale in the bandwidth of 5–200 mm covering the variability in annual sedimentation rate (e.g., varve thickness). Vertical axis: logarithmic scaled wavelengths (periods). The signal variances are represented by the darkness of the gray value (white = <25% of maximum variance, light gray <50% of maximum variance, dark gray, 75% of maximum variance, black = >75% of maximum amplitude) in the scalogram. Note that the sedimentary cycles have fluctuating intensity and wavelengths.

Table 2. Recovered synthetic signals in time scale T_i.

Raw (i)	Time (yr. BP) T_i	Varve thickness $v(t)$	Image color $x(t)$
1	0.13	58.48	116.94
2	0.38	58.48	114.68
3	0.63	58.48	121.11
4	0.88	58.48	116.76
$i = 5$	T_5	v_5	x_5
$i = 5$	T_i	v_i	x_i
$i = 1962$	T_{1962}	v_{1962}	x_{1962}
1963	490.63	58.48	108.98
1964	490.88	58.80	108.20
1965	491.13	62.47	106.00
1966	491.38	62.87	106.83
$n = i = 1967$	491.63	62.87	110.13

i with a simple linear interpolation algorithm (Table 2). The recovered time series $x(t)$ and $v(t)$ are the results of this transform, which, ideally, should be exact replicas of the synthetic signals (Figs. 5D and E), respectively.

Discussion of the result of the transform

Visual comparison of the recovered time series with original synthetic signals (Fig. 7B, C, E) show that the amplitude, mean, and phase at $t = 0$ are very similar. Differences are; (i) the 1.8% shorter recovered time-series and the slightly shorter ~20 year cycle lengths in $x(t)$ and $v(t)$ which are directly connected with the time-scale, (ii) the recovered sedimentation rate cycles, which are less sinusoidal but rather binary, and (iii) the occurrence of an outlier in the sedimentation rate (~80 mm/year at ~300 yr. BP) (Fig. 7E).

Wavelet analysis (Fig. 7A, D) show very sharp 20–year cycle bands both in climate signal (i.e., image color) and sedimentation rate, respectively. In particular the ~10 year interference signal (Fig. 6B) is absent, and the annual cycle band narrows to ~0.9–1.1 years (Fig. 7A).

Spectral analyses of the original and recovered synthetic signals (Fig. 8) show that the cycle bandwidths are virtually identical. In particular, the widened annual 37–62 mm spectrum and the artificial ~400 mm (10 year) cycle, that occurred in the depth scale, is narrowed by the time-series recovery. Spectral analysis separated two variance peaks for the annual cycle in the original synthetic data (Fig. 8B). The annual cycle band in the recovered data also ranges from ~0.95–1.05 years but with more, smaller peaks (Fig. 8E).

In summary, the depth-to-time scale transform methodology proposed is able to:

1) Extract (recover) sedimentation rate and sediment color time-series correctly in amplitude and phase from a single sediment color depth series (image data), if the sedimentation rate fluctuates in well-defined bandwidths (e.g., restricted range of laminae thickness).

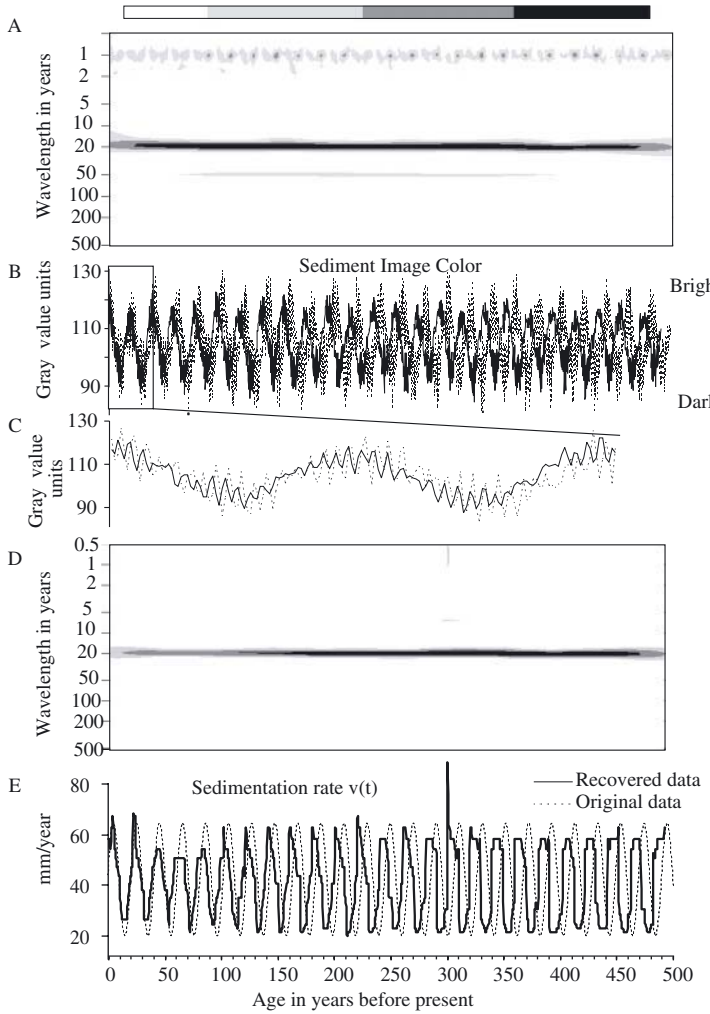

Figure 7. Wavelet analysis of recovered synthetic signals in time-scale; A: Scalogram of the recovered image color in time-scale. Note the narrow variability of the annual cycle, and occurrence of 20 year and weak 50 year cyclicity, as well as low influence of edge effects. For explanation of gray scale bar on top see Figure 6C; B: Overlay of recovered and original synthetic signals in time scale. Note the slight phase shift between the two series due to a shortened recovered time-series (492 instead of 500 years); C: 40-year zoom into original and recovered synthetic sediment image color signals. Note that the original variability between low contrast and high contrast "varves" is preserved in the recovered synthetic signals; D: Scalogram of the recovered sedimentation rate in time-scale. Note the narrow variability of 20-year cyclicity. For explanation of gray scale variations see Figure 6C; E: Overlay of synthetic recovered and original sedimentation rate signals. Note the artificial spike up to ~80 mm at 300 year BP, and slight artificial variability in amplitude.

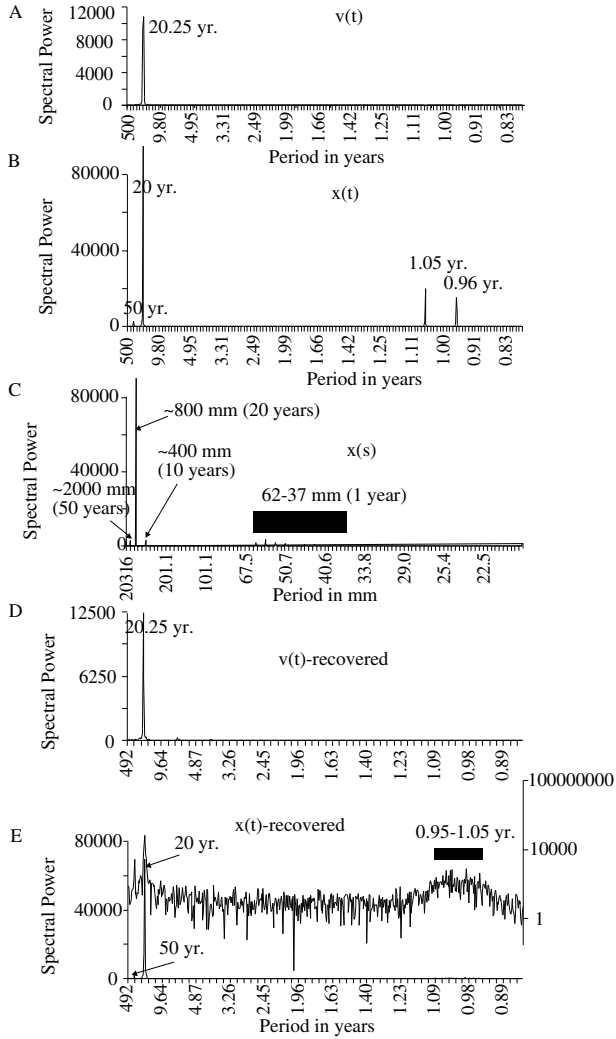

Figure 8. Spectral analysis (periodograms) of synthetic signals (see Figs. 5, 6); A: from synthetic sedimentation rate in time-scale (Fig. 5E); B: from synthetic sediment image color in time-scale; note the double peak for annual signal; C: from synthetic time-series in depth scale generated from sedimentation rate modulated periodic signals and noise (Fig. 6A); note artificial ~400 mm cycle (~10 years) and broad band of annual cycle (37–62 mm). Black bars indicate ranges of significant period bands; D: from recovered synthetic sedimentation rate signals in time-scale; note the sharpness and same variance of the 20 year peak as in original synthetic data (Fig. 5A); E: from recovered synthetic sediment image color signals in time-scale, note the similarity in the variance of the 20 year and 50 year peak as in original data, as well as the broad, and wide band of low-variance annual cyclicity. Bold line: linear scaled periodogram; fine line: logarithmic scaled periodogram.

2) Compare quantitatively both sedimentation rate and sediment color, because the recovered time series are related to exactly the same time scale.

3) Separate cycles in sedimentation rate and sediment color at the correct (original) amplitude, without interference signals even if their wavelengths are identical.

Extract correct sedimentation rates and sediment colors even when there is a low contrast between laminae and the background signal.

As a drawback, bandwidth errors, edge effects and other analytical uncertainties can provide (1) ~2% errors in bandwidth that can result in shortened or lengthened time-scales, and (2) artificial outlier values in sedimentation rate.

In addition, laminae that are less than two pixels wide, completely missing time intervals, or intervals that are related to non-deposition or erosion will not be represented in the time-scale. However, the location of missing laminae can often be detected by wavelet analysis over the entire spectrum, because of the occurrence of abruptly shifting gray and black bands in the scalograms (Prokoph and Agterberg 2000).

Example: Marine Laminated sediments from the west coast of Vancouver Island, NE Pacific

Geological and technical background

An ~11 m sediment core was collected in 1999 from Effingham Inlet, SW Vancouver Island, British Columbia to investigate the climate and oceanographic variability in the NE Pacific over the last ~5000 years. The laminae consist of dark, mineral-rich layers (winter layers) and diatom-rich spring-summer layers. X-ray images of 20 cm-slabs of the sediment core were taken and digitized in a resolution of 116 pixel/cm. The example documents the analysis and depth to time scale transform of a 37 cm long section (873–910 cm depth) that is composed of annual lamination in various thickness, contrast and gray levels (Fig. 9E). The top of the section is estimated to have been deposited at ~3800 yr. BP. Three pixel wide line-scans were extracted from the X-ray images using program IMAGEJ after background calibration (e.g., Nederbragt and Thurow (2001)).

Time-scale construction

The wavelet analysis over the complete wavelength-spectrum reveals a strong cycle band in the range of ~0.15–0.4 cm (Fig. 9A) that is overlaid by relatively weak ~0.8 cm, ~1.2 cm, and ~2.5 cm cycles at the top. Extraction of the three most intense wavelengths $a_{\mathrm{Wmax}(b)}$ (Fig. 9C) shows that the ~0.15–0.4 cm cycle band can be traced through the section. Visual comparison also indicates that this wavelength band reflects the mean annual sedimentation rate or varve thickness.

(2) Narrow-band wavelet analysis (Fig. 9B) in the annual bandwidth for $k = 1000$ intervals (i.e., Δs = (960–873 cm)/1000 = 0.037 cm), shows that the varves are thickest at ~883–897 m depth.

(3) Using these cycle lengths as proxies of sedimentation rate v_k, the time-scale is calculated according to eq. (5) (Table 3). The age at the top t_0 is approximately 3800 years before present (Patterson et al. 2001). The transform extracts 137 annual laminae providing

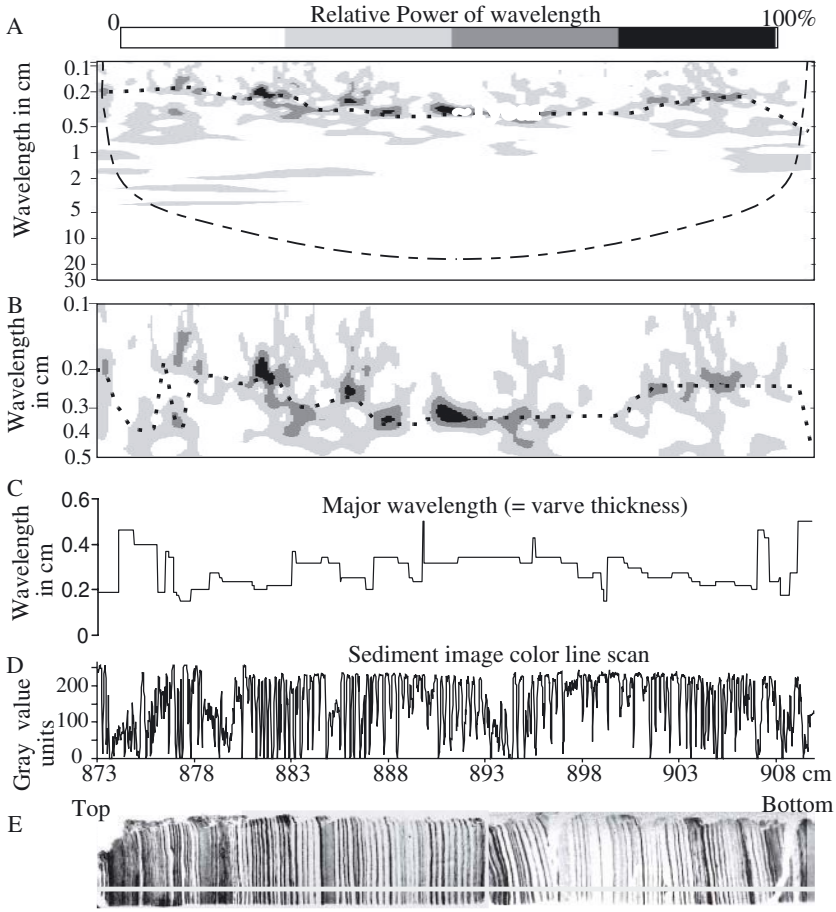

Figure 9. Wavelet analysis of sediment color (in gray scale) data from two X-ray images from a representative section 873–910 cm depth of core TUL99B03. The time-series of the two core-slabs has been connected at 893 cm depth; A: Wavelet analysis over complete spectrum, the excellent preservation of the annual cycle of fluctuating thickness (∼0.15–0.4 cm); B: Narrow band wavelet analysis of 0.15–0.5 cm bandwidth; C: Major wavelength (strongest local wavelet coefficients) at each location; D: Digitized sediment color line-scan (∼4,000 data points), the gray-values range from 0 (black) to 255 (white); E: X-ray image with digitized line-scan (horizontal gray line).

an age range of the complete interval of 3800–3937 years before present. In the next step, mean sediment gray value data $x(s)$ are calculated using MITTELN.C for the depth intervals $\Delta s = 0.037$ cm of the wavelet analysis output forming x_k.

(4) The time intervals t_k are then transformed to $i = 685$ equal time-intervals $\Delta t = 0.2$ years using MITTELN.C. Then, ν_k and x_k are transformed for the same time intervals to ν_i and x_i using MITTELN.C, respectively. Consequently, the data sets of sedimentation

Table 3. Wavelet transform output of narrow-band analysis of X-ray data.

Raw (k)	Depth (mm)	$W_{\max(b)}$ varve thickness	Age (years)
	873.00		$T_0 = 3800$
1	873.04	0.19	3800.20
2	873.07	0.19	3800.39
3	873.11	0.19	3800.59
4	873.15	0.19	3800.79
$k = 5$	s_5	v_5	T_5
k	s_k	v_k	T_k
$k = 995$	s_{995}	v_{995}	T_{995}
996	909.85	0.50	3936.72
997	909.89	0.50	3936.79
998	909.93	0.50	3936.86
999	909.96	0.50	3936.94
$m = k = 1000$	910.00	0.50	3937.01

rate (varve thickness) and sediment gray values are transformed into time scale of equal time interval $\Delta t = 0.2$, forming the time-series $v(t)$ and $x(t)$ respectively (Fig. 10B, D).

The horizontal alignment of high wavelet coefficients in the sediment color time-series in the annual cycle band (black and dark-gray bands in Fig. 10A) indicates that the time-intervals are indeed well equalized, compared to the depth-series (Fig. 9).

Palaoenvironmental interpretation of time-series

The wavelet coefficient >25% maximum variance in varve thickness form a persistent 11 years cyclicity (Fig. 10C) that is not detectable from the depth-series (Fig. 9). The ~11 year wavelength could be related to ~11 year sunspot ("Schwabe") cycle (Friis-Christensen and Lassen 1991). For further filtering and modelling purposes, these two period bands and their amplitudes can be extracted and used as input parameter for periodic data driven models of sediment accumulation. The sediment color variability is dominated by the annual variations. A short-term ~10 cyclicity appears over ~40 years (= four cycles) on the top and may indicate a temporary influence of sunspot activity on mineralogical and biotic composition of the sediment.

Summary

High-resolution time-scales are important for the precise correlation of spatially distributed geological records, and further development of process-oriented models used to predict climate change and other terrestrial processes. The extraction of digital line-scan data from images of laminated sediments provides a tool for the rapid and non-invasive analysis of sedimentary records, including sediment and ice cores, and tree ring growth patterns.

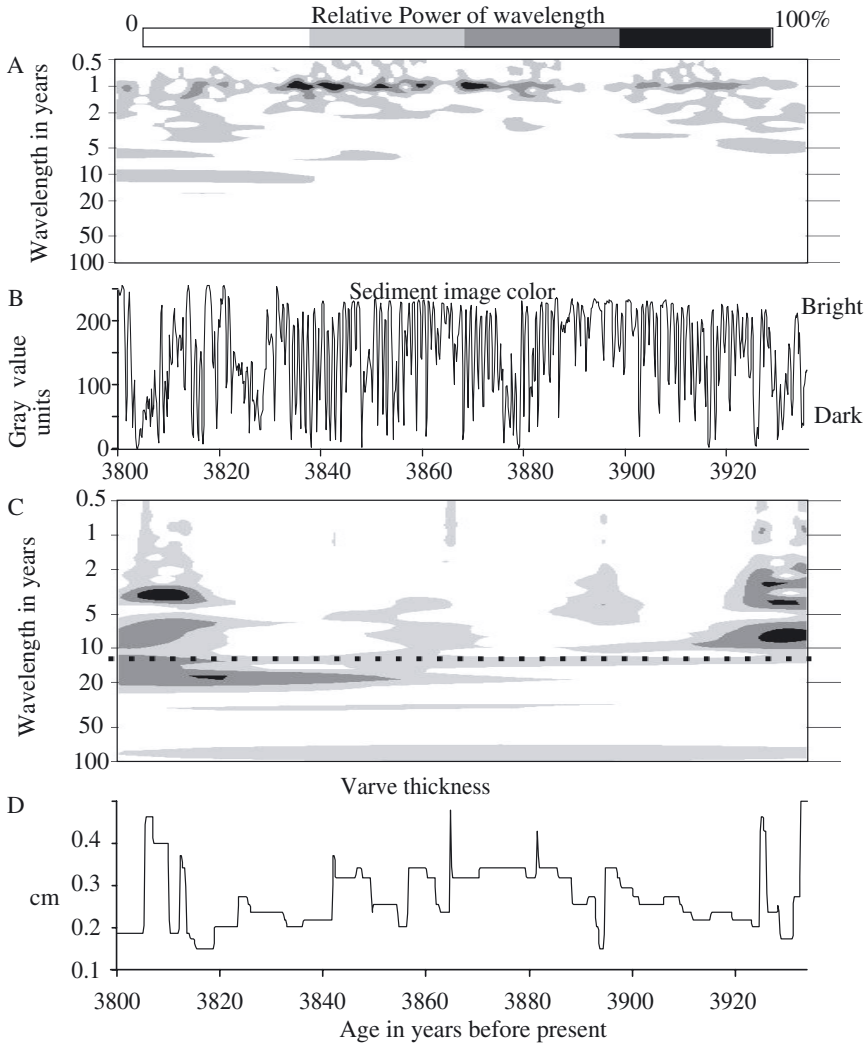

Figure 10. Wavelet analysis of recovered image color and varve thickness data in time-scale from 873–910 cm depth of core TUL99B03; A: Scalogram of sediment image color, note the excellent and narrow band preservation of the annual cycle and ~10-year cyclicity at the top; B: Recovered sediment image color time series in time scale in 0.2-year resolution; C: Wavelet analysis of varve thickness, note the persistent and narrow band preservation of a ~11-year cyclicity (dotted line); D: Recovered varve thickness time series (0.2-year time scale).

The four-step semi-automatic methodology is based on wavelet and other transform to transform digital line-scan image data from obtained laminated sedimentary successions, from a depth-scale into a time-scale using narrow-band wavelet analysis with Morlet wavelet as the "mother" function, and additional linear transforms and interpolation algorithms. Using the same method high-resolution time-series of lamination (i.e., varve) thickness and sediment color are extracted, providing useful information on paleoenvironmental fluctuations during the sedimentation.

With this methodology, it is possible to (1) extract temporal variability in sedimentation rate and climate proxy signals (e.g., image color, mineral composition) even if the wavelengths of the signals overlay each other, (2) extract a high-resolution time scale, and (3) extract original temporal variability in periodicity, abrupt changes and phase shift with ∼2% accuracy error. Furthermore, it is possible to connect samples (e.g., geochemical, paleontological) taken from the sedimentary section precisely to the constructed time-scale.

The extraction of high-resolution time-scales using variations in image colors from laminated sediments is only dependent on:

- the presence of a well-defined extraterrestrial periodic cyclicity (e.g., annual rotation of the Earth around the sun) in the entire sedimentary succession to be analyzed,
- continuity of this signal in the digitised sediment image or succession of images,
- a requirement for at least 4 data points (pixel) covering the thinnest lamina, and
- the requirement of one or more tie-ages (e.g., radiocarbon dating) to fit the relative counts into an absolute time-scale.

Acknowledgments

This research was supported by a Natural Sciences and Engineering Research Council of Canada strategic project grant to RTP. We thank E. Verrecchia, P. Francus, and two anonymous reviewers for their suggestions and careful evaluation of the manuscript.

References

Appenzeller C., Stocker T.F. and Anklin M. 1998. North Atlantic oscillation dynamics recorded in Greenland ice cores. Science 282: 446–449.

Berger A., Loutre M.F. and Dehant V. 1989. Influence of the changing lunar orbit on the astronomical frequencies of pre-Quaternary insolation patterns. Paleoceanography 4: 555–564.

Chao B.F. and Naito I. 1995. Wavelet analysis provides a new tool for studying Earth's rotation. EOS 76: 164–165.

Frakes L.A., Francis J.E. and Syktus J.I. 1992. Climate Modes of the Phanerozoic: the History of the Earth's Climate Over the Past 600 Million Years. Cambridge University Press, Cambridge, U.K., 274 pp.

Friis-Christensen E. and Lassen K. 1991. Length of the solar cycle: An indicator of solar activity closely associated with climate. Science 254: 698–700.

Gedalof Z. and Smith D.J. 2001. Interdecadal climate variability and regime-scale shifts in Pacific North America. Geophys. Res. Lett. 28: 1515–1518.

Gradstein F.M. and Agterberg F.P. 1998. Uncertainty in stratigraphic correlation. In: Gradstein F.M., Sandvik K.O. and Milton N.J. (eds), Sequence Stratigraphy: Concepts and Applications. Elsevier, Amsterdam, pp. 9–29.

Grossman A. and Morlet J. 1984. Decomposition of Hardy functions into square integrable wavelets of constant shape. SIAM J. Math. Anal. 15: 732–736.

Hays S.D., Imbrie J. and Shackleton N.J. 1976. Variations in the Earth's orbit: Pacemaker of the ice ages. Science 194: 1121–1132.

Milankovitch M. 1941. Kanon der Erdbestrahlung und seine Anwendung auf das Eiszeitproblem. Serbian Academy of Science, Belgrade 133, 633 pp.

Misiti M., Misiti Y., Oppenheim G. and Poggi J.-M. 1996. Matlab Wavelet Toolbox User's Guide. The Mathworks, Inc. Mass.

Morlet J., Arehs G., Fourgeau I. and Giard D. 1982. Wave propagation and sampling theory. Geophysics 47: 203.

Nederbragt A.J. and Thurow J. 2001. A 6,000 year varve record of Holocene sediments in Saanich Inlet, British Columbia, from digital sediment colour analysis of ODP Leg 169S cores. Mar. Geol. 174: 95–110.

Patterson R.T., Prokoph A., Dallimore A., Thomson R.E., Ware D.M. and Wright C. 2001. Impact of abrupt Holocene climate changes and solar cyclicity on fish population dynamics in the NE Pacific. GSA annual meeting, Boston, USA, Paper No. 65–0.

Prokoph A. and Barthelmes F. 1996. Detection of nonstationarities in geological time series: Wavelet transform of chaotic and cyclic sequences. Comp. Geosci. 22: 1097–1108.

Prokoph A. and Agterberg F.P. 2000. Wavelet-Analysis of Well-Logging Data from Oil Source Rock, Egret Member, Offshore Eastern Canada. AAPG Bulletin 84: 1617–1632.

Rioul O. and Vetterli M. 1991. Wavelets and Signal Processing. IEEE Special Magazine: 14–38.

Torrence C. and Compo G.P. 1998. A Practical Guide to Wavelet Analysis. Bull. Amer. Meteor. Soc. 79: 61–78.

Schaaf M. and Thurow J. 1994. A fast and easy method to derive highest-resolution time-series datasets from drillcores and rock samples. Sed. Geol. 94: 1–10.

Schwarzacher W. 1993. Cyclostratigraphy and Milankovitch Theory. Developments in Sedimentology 52. Elsevier, Amsterdam, Netherlands, 225 pp.

Varem-Sanders T.M.L. and Campbell I.D. 1996. Dendroscan: a Tree-Ring Width and Density Measurement System. Special Report 10, Canadian Forest Service Centre. UBC Press, Vancouver, Canada, 131 pp.

Ware D.M. and Thomson R.E. 2000. Interannual to Multidecadal Timescale Climate Variations in the Northeast Pacific. J. Climate 13: 3209–3220.